



Instrument Science Report WFC3 2007-026

WFC3 TV2 Testing: UVIS-2 Dark Frames and Rates

A.R. Martel
November 02, 2007

ABSTRACT

WFC3 underwent its second thermal vacuum testing in the Space Environment Simulation Chamber at the Goddard Space Flight Center over the summer and fall of 2007. Throughout this campaign, dark frames were acquired for the spare UVIS-2 detector at several operating temperatures. In all the long dark frames (3000 sec), a “hot” spot is detected at the top of the A and B quadrants. The dark rate at -81.6 C (gain=1.5 e⁻/DN) is ~0.1 e⁻/hour/pix and at -78.2 C (gain=1 e⁻/DN), ~ 0.55 e⁻/hour/pix. The AB chip has a higher dark current rate and a greater fraction of hot pixels than the CD chip, by factors of 1.6 and 1.2 respectively. Quadrant B exhibits the worse behavior: it has the highest dark current rate, the largest fraction of hot pixels, and the highest mean hot pixel rate, more than twice the rate of the other quadrants. Quadrant C has the lowest dark rates. The dark current rates are consistent with the well-known dark current equation from -81.6 C to -3.6 C. The dark current rate easily meets the CEI specification for temperatures colder than -54 C.

Introduction

The acquisition of dark frames represents an important part of the on-orbit calibration activities of HST. These frames serve to monitor the dark current rate, the growth of hot pixels from radiation damage, and to produce superdark reference files for the pipeline. It is therefore crucial to obtain dark frames on the ground in the most common configuration of the detector to serve as a comparison baseline for the on-orbit darks, to

understand the behavior of the dark current and verify if it meets the specifications of the Contract-End-Items (CEI), and to deliver pre-launch reference files. Such dark frames were obtained for the backup UVIS-2 detector (CCD40 – amplifiers C and D, CCD50 – amplifiers A and B) of WFC3 as part of the Thermal Vacuum 2 (TV2) campaign at the Goddard Space Flight Center (GSFC) in the summer and fall of 2007. In the following, we present an analysis of these dark frames.

The Data

In Table 1, we list the dark frames included in this study (Appendix A). Only the frames at the cold temperatures of -81.6 C and -78.2 C were acquired as part of dedicated SMSs (UV01S03A, UV01S01A, and UV01S13), the remainder coming from the imaging portion of the Servicing Mission Functional Test or from the Aliveness Test at the warm temperature of the detector at the time of execution. No dark frames were acquired at the nominal on-orbit temperature of the detector (-83 C) due to a lien against the TECs. Only full frames with the standard four amplifier readout (ABCD) and a binning of 1x1 are considered. Sufficient data are available only for commanded gains of 1 and 1.5 e⁻/DN. We make no distinction between MEB Sides 1 and 2; any effect from the different electronic boards on the dark current rates is likely much smaller than variations caused by the detector temperature. Frames acquired in special modes, such as charge injection and post-flash, are excluded, as well as frames that show the signature of hysteresis, in particular the "bowtie" anomaly (Bushouse & Lupie 2005) and PSF spots from the alignment verification.

Analysis

Image Processing

All dark frames were processed with a Python class written by one of us (Martel). A linear fit through the serial virtual overscan region was first subtracted from each quadrant. The dark frames at a given detector temperature were then combined either as a median for three or more images, a mean for two images, or no combination for a single image. Bias frames acquired at the same temperature, amplifier readout, and commanded gain as the dark frames, and acquired as close as possible in time (usually within the same SMS), and showing consistent levels (see below) were processed in a similar way and subtracted from the assembled dark frames. This last step removes the signature of fixed pattern noise in the peak of the dark current histograms and thus greatly improves the calculation of the mode.

Dark Rate Calculation

Several methods can be used to calculate the dark current rate with different degrees of accuracy. A simple mean or median over the entire field or over the individual quadrants, or a Gaussian fit to the entire dark current distribution, will usually overestimate the dark current rate because of the bias introduced by the hot pixel tail. To avoid this, the hot pixel tail is sometimes reduced with sigma-clipping. More empirical methods include modeling the dark current histogram with a log-normal Gaussian or with a Gaussian and an exponential drop-off for the tail.

For WFC3 UVIS, we simply calculate the mode of the histogram of the counts using a Gaussian fit while excluding the hot pixel tail. Our Python script offers the option of fitting the Gaussian above a certain fraction of the peak to avoid the contribution of the hot pixels. At cold operating temperatures (-81.6 C or -78.2 C, for example), this level is very low, about 0.1% of the peak (see Fig. 2). At warmer temperatures, the hot pixel tail becomes significant (Fig. 3) and so the user can specify only a portion of the right wing of the main peak to include in the fit. We note that this approach is very similar to that used by the ACS team to calculate the on-orbit dark rate of the Wide Field Channel (M. Sirianni, private communication).

In general, the dark frames acquired in this campaign are not deep and so the Poissonian shot noise on the dark current is large. This is particularly true at cold temperatures at which the dark current is small and barely above the bias level. For multiple frames at a given temperature, we choose the error on the mean as the uncertainty on the final measurement; otherwise, for single frames, we assume an uncertainty of 10%.

Results

The Dark Frames

The median dark images at gain=1.5 e⁻/DN are shown in Fig. 1 for operating temperatures of -3.6 C, -53.9 C, and -78.2 C after subtraction of a matching median bias frame. The warmest dark (-3.6 C) shows a periodic, diagonal striation pattern in the general orientation of the Amp B to Amp C axis. The dark frame at -53.9 C is smooth and shows no discernible structure. On the other hand, the cold dark frame at -78.2 C shows four curious enhancements along the vertical edges of each quadrant as well as at the top of quadrants A and B. The four vertical regions are faint and appear roughly semi-circular in shape and protrude from the edges, extending towards the center along the central third of the quadrants. A horizontal slice through the quadrants shows that the

counts rise slowly, starting ~ 700 pixels from each edge, up to about twice the counts in the central part of the quadrant. The enhancement at the top of quadrants A and B is slightly brighter and more flattened and is offset so that most of it lies on the Amp A quadrant.

To investigate further the nature and origin of these edge enhancements, we examined the raw dark frames and the bias frames. All five features are present in the individual dark frames that were combined to produce the median dark at -78.2 C. Hence, they were not introduced by the bias frame subtraction. Moreover, the four vertical features are absent in the median dark frames at -78.2 C (gain=1) as well as at -81.6 C (gain=1.5). These are also long integrations of 3000 sec. But the Amp AB horizontal feature is obvious in the -81.6 C (gain=1.5) and -78.2 C (gain=1) darks, suggesting that the origin of this feature is different from the four others. None of the features are observed in the -53.9 C darks, possibly because of their relatively short integration times (100 sec).

None of the bias frames show any of the five edge features found in the darks. Instead, the median biases possess two wide vertical side bars, roughly 800 pixels in width, along the outside edges of the C and D quadrants (Fig. 2). These are present in all the median biases. We also examined several other bias frames acquired throughout the entire TV2 campaign and the bars are present in all of them. These features are therefore intrinsic. The A and B quadrants are comparatively clean. The level of the side bars is roughly twice that of the central part of the quadrant. The side bars are also visible in the individual, raw dark frames but not in the final median dark frames, indicating that the full-frame bias subtraction is effective in removing them.

The nature of the four enhancements along the vertical edges of the median dark frame at -78.2 C and gain=1.5 e^-/DN is unknown. Amplifier glow, which might be expected in such long integrations, can probably be dismissed since the features are not located in the corners of the four read-out amplifiers. In fact, the features are very reminiscent of the so-called "bowtie" (Bushouse & Lupie 2005), albeit a very weak example which would have easily eluded our initial verification. This anomaly was observed in TV1 with the UVIS-1 detector and in darks and internal flat fields in TV2 and so appears common to the WFC3 CCDs. Its origin and nature are unknown. No systematic pattern has been found to explain its occurrence and attempts to reproduce it have so far been unsuccessful.

The enhancement at the top of Amps A and B is also difficult to explain, although perhaps more tractable. Baggett & Hilbert (2004) noticed this feature in dark frames acquired in Jan 2003 - Dec 2004 while the instrument was in the ambient environment of the Spacecraft Systems Development and Integration Facility (SSDIF) at GSFC but for the UVIS-1 detector. They attributed the feature to stray light from the clean room coming through a leak in the instrument. This interpretation is difficult to reconcile with the light-tight environment of the vacuum chamber in TV2. We note that contamination from the internal calibration lamps is not the culprit: the instrument telemetry indicates that all five lamps were off during the TV2 dark frame integrations.

External illumination by the external CASTLE stimulus through the normal UVIS light path, although unlikely, could also be a source of contamination. Typically, before executing an SMS of dark frames, the operator of the Calibrated Stimulus from Leftover Equipment (CASTLE) runs a preparation script to close the CASTLE dark shutter, shut off all laser sources, and to close the monochromator. This effectively cuts off all CASTLE lamp sources. But if the CASTLE operator is not informed that an all-dark SMS is upcoming, he/she might not run the preparation script and a lamp might be left on from the previous SMS. Examining the log files, we find that the long darks were preceded by SMSs that made use of CASTLE, in particular flat fields to measure the gain and UVIS and IR science monitors. At our request, R. Telfer verified the status of CASTLE during execution of the dark frame SMSs. He finds that all CASTLE light sources were off for the -78.2 C (gain=1.5) and -81.6 C (gain=1.5) dark frames but that CASTLE was still configured to the last exposure (a 1050 nm point source) of the IR science monitor for the -78.2 C (gain=1) darks. Hence, we conclude that CASTLE illumination is not the cause of the features seen on the long dark frames. As a precaution in future calibration campaigns, it will be important to inform the CASTLE operator of any all-dark SMS so that CASTLE can be configured correctly.

We conclude that the feature at the top of quadrants A and B is not due to illumination from stray light, either from an external CASTLE source or from the internal calibration lamps. It may simply be a true "hot" spot intrinsic to the CCD perhaps resulting from a peculiarity in the coupling of the CCD to the TECs or from the manufacturing process of the CCD.

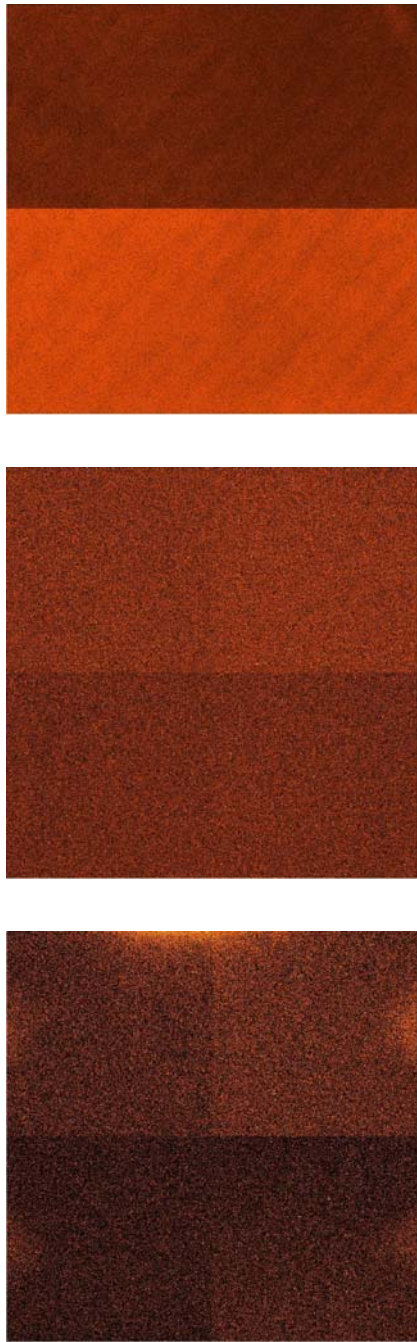


Figure 1: WFC3 UVIS-2 median dark frames after full-frame bias subtraction at -3.6 C (top), -53.9 C (middle) and -78.2 C (bottom) and gain=1.5 e⁻/DN in standard orientation (amp A in top-left corner and amp D in bottom-right corner). The images are expressed in e⁻ and binned 5x5. All overscan regions have been trimmed.

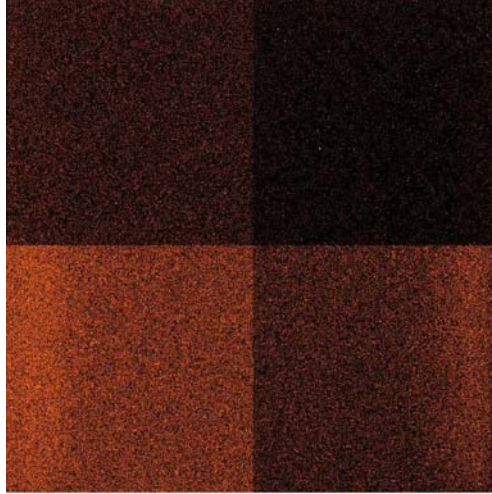


Figure 2: WFC3 UVIS-2 median bias frame at -78.2 C and gain=1.5 e⁻/DN. The vertical bars along the Amps C and D edges can be seen. The image is in e⁻ and binned 5x5.

The Dark Current Rate

The dark current rates for the cold temperatures of -81.6 C (gain=1.5) and -78.2 C (gain=1) are tabulated in Table 2. The dark rates for the -78.2 C (gain=1.5) frames are not considered because of the contamination by the vertical edge anomalies. As an example of our analysis, the dark count histograms at -78.2 C (gain=1) for each amplifier are shown in Fig. 3. The weighted mean rates for all four amplifiers are: 0.082 e⁻/hour/pix (-81.6 C, gain=1.5) and 0.54 e⁻/hour/pix (-78.2 C, gain=1). These are well below the CEI specification of < 20 e⁻/hour/pix.

Table 2. Dark Current Rate in e⁻/hour/pix

Amplifier	-81.6 C (gain=1.5)	-78.2 C (gain=1)
A	0.104 ± 0.096	0.656 ± 0.043
B	0.150 ± 0.086	0.666 ± 0.134
C	0.007 ± 0.323	0.420 ± 0.087
D	0.133 ± 0.308	0.496 ± 0.047

Note: The rates apply to the standard four-amp readout (ABCD) and binning of 1x1. The conversion from counts to electrons is made using the gains tabulated in Baggett (2007): 1.57, 1.54, 1.63, and 1.59 e⁻/DN for gain=1.5 and 1.07, 1.07, 1.11, 1.08 e⁻/DN for gain=1.

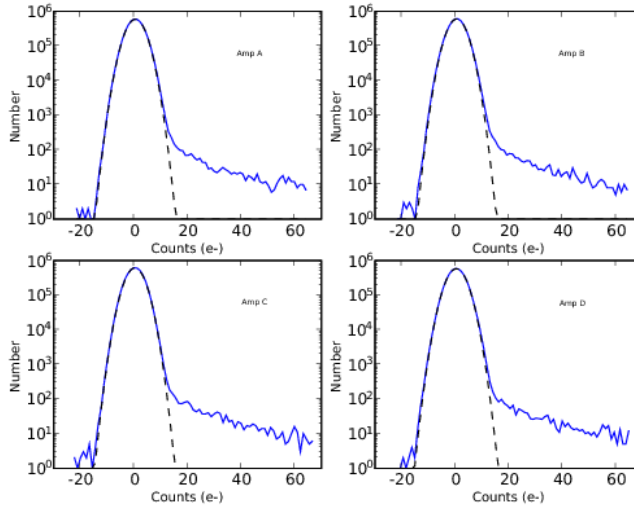


Figure 3: Histograms of the counts in each quadrant of the median dark frame at a temperature of -78.2 C (gain=1). The dashed line is the Gaussian fit to the peak.

The Hot Pixels

The population of hot pixels can be analyzed when the median frame can be assembled from three or more dark frames to insure a robust removal of cosmic-ray hits, which particularly affect the longest exposures (3000 sec). For a detector temperature of -78.2 C, we define hot pixels as those with a count rate of ≥ 30 e⁻/hour/pix, well away from the main Gaussian peak. This value is arbitrary and should be increased for warmer temperatures.

In Table 3, the fraction of hot pixels in each quadrant and their mean count rates are listed for a temperature of -78.2 C (gain=1). Although these values were calculated after a full-frame bias subtraction, we find nearly identical numbers if the hot pixels are characterized on the overscan-subtracted images only. The AB chip has more hot pixels than the CD chip, by a factor of about 1.2. Moreover, quadrant B not only has the highest fraction of hot pixels but also the highest mean hot pixel count rate, more than twice the rate of the other quadrants.

Table 3. Hot Pixel Fraction and Mean Count Rate (-78.2 C, gain=1)

Amplifier	Fraction (%)	Mean Rate (e⁻/hour/pix)
A	0.0236	110
B	0.0258	230
C	0.0212	85
D	0.0207	85

The Temperature Dependence

A search of the WFC3 database reveals that several dark frames were acquired at "warm" temperatures throughout the TV2 campaign (see Table 1 : -3.6 C, -5.8 C, -7.5 C, -7.9 C, and -53.9 C). We can therefore perform a rough analysis of the behavior of the dark rate with temperature. In Fig. 4, we plot the distributions of the dark rates for four of these warm temperatures. As expected, the growth of the hot pixel tail and the increase in the dark current rate, as indicated by the shift of the main peak towards higher counts, are extremely sensitive to the temperature. The periodic bumps in the dark rate distributions at the warmest temperatures are likely due to the broad striations in those dark frames (see the -3.6 C frame in the top panel of Fig. 1, for example).

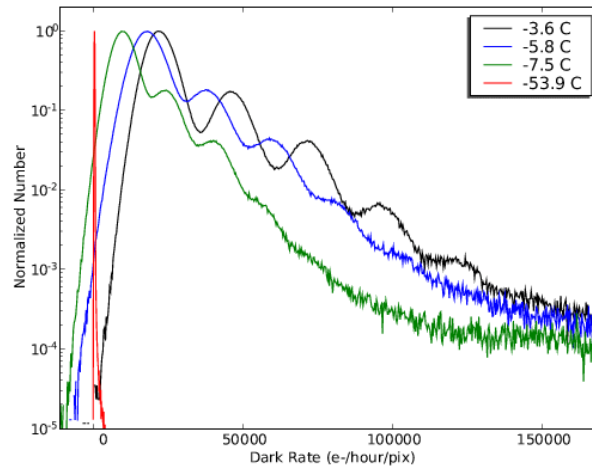


Figure 4: Distributions of the dark count rates at warm temperatures normalized to their peak values (amp A only).

The dark rates measured at the warm temperatures are listed in Table 4 for each amplifier. At a temperature of -53.9 C, our results agree very well with those of Hilbert (2007) who measured the dark rates for the same detector when the instrument was in ambient environment in SSDIF in preparation for TV2. Like them, we also find that amplifier B has the highest dark rate while amplifier C, the lowest. In fact, within the uncertainties, this appears to be true for all temperatures (see also Table 2). Comparing the dark rates between the two chips at all temperatures, the AB chip has a significantly higher dark rate than the CD chip, typically by a factor of ~ 1.6 . The dark current rate meets the CEI specifications at temperatures colder than -54 C.

Table 4. Dark Current Rate at Warm Temperatures in $e^-/\text{hour}/\text{pix}$ (gain=1.5)

Amplifier	-53.9 C	-7.9 C	-7.5 C	-5.8 C	-3.6 C
A	12.0 ± 2.2	7070 ± 710	9685 ± 970	17920 ± 1790	21825 ± 2120
B	12.2 ± 1.5	7015 ± 700	9775 ± 980	18905 ± 1890	22805 ± 2160
C	6.7 ± 1.0	4130 ± 410	6070 ± 610	12305 ± 1230	15020 ± 1380
D	7.7 ± 1.1	4065 ± 410	6130 ± 610	13065 ± 1310	15690 ± 1580

We can verify that our measurements behave as predicted by the dark current equation (Janesick 2001). This expression is D_R (e⁻/hour/pix) = 3600·C·T^{1.5}·exp(-E_g/2kT) where C is a constant, T is the operating temperature in Kelvins, E_g is the silicon bandgap energy in eV, $E_g = 1.1557 - 7.021 \times 10^{-4} \cdot T^2 / (1108 + T)$, and k is Boltzmann's constant (8.62 × 10⁻⁵ eV/K). The equation only needs to be solved for the scaling factor C. The fits are shown in Fig. 5 for the two chips; the measurements agree generally well with the model except for amp C at -81.6 C which shows an unusually low dark current rate.

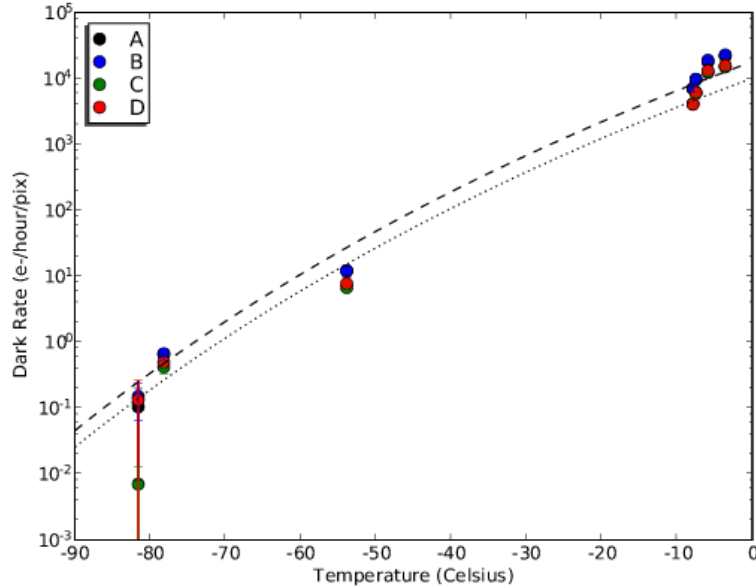


Figure 5: The dark rate measurements (gain=1.5) for the UVIS-2 detector are modeled with the dark current equation (dashed line: amps AB, dotted line: amps CD).

Conclusions

We have measured the dark current rate for the UVIS-2 detector of WFC3 at several operating temperatures. The dark current rate meets the CEI specification for temperatures colder than -54 C and behaves as predicted by the dark current equation from -81.6 C to -3.6 C. The AB chip exhibits a higher dark rate and a larger fraction of hot pixels than the CD chip, by factors of about 1.6 and 1.2 respectively. Quadrant B has the worse behavior of all four quadrants: it has the highest dark rate and the largest fraction and rate of hot pixels.

Acknowledgements

I thank S. Baggett for early comments and advice in the preparation of this document.

References

- Baggett, S. & Hilbert, B. 2004, ISR 2004-01, "Readnoise and Dark Current in WFC3 Flight CCD Ambient Data"
- Baggett, S. 2007, WFC3 ISR 2007-19, "WFC3 TV2 Testing: UVIS2 Gain Results"
- Bushouse, H., & Lupie, O. 2005, WFC3 ISR 2005-20, "WFC3 Thermal Vacuum Testing: UVIS Science Performance Monitor"
- Hilbert, B. 2007, WFC3 ISR 2007-10, "WFC3 Ambient Testing: UVIS Dark Current Rate"
- Janesick, J.R. 2001, Scientific Charge-Coupled Devices, SPIE Press, p. 622

Appendix A.

The OPUS-processed WFC3 UVIS-2 dark frames used to calculate the dark current rate are listed below. The frames were acquired on either Side 1 (MEB1) or Side 2 (MEB2) in the standard four-amp readout mode (ABCD), a binning of 1x1, and a commanded gain of 1.0 or 1.5 e⁻/DN. The operating temperature of the detector is taken from the IUVDTEMP header keyword.

Table 1. Dark Frames in Thermal Vacuum 2 Campaign

File Name	ID	Observation Date	MEB	Gain (e ⁻ /DN)	Temperature (Celsius)	Integration Time (sec)
i9v9w202r_07173161632_raw.fits	30122	2007/06/22	2	1.5	-3.6	20
i9v9w202r_07189151527_raw.fits	34080	2007/07/08	1	1.5	-3.6	20
i9v9w202r_07189011623_raw.fits	34070	2007/07//08	2	1.5	-5.8	20
i9v9w202r_07173053950_raw.fits	30108	2007/06/22	1	1.5	-7.5	20
i9v9w202r_07203085925_raw.fits	37405	2007/07/22	1	1.5	-7.9	20
i61gm302r_07162151231_raw.fits	29074	2007/06/11	1	1.5	-53.6	100
i61gm304r_07162153120_raw.fits	29075	2007/06/11	1	1.5	-54.0	100
i61gm302r_07163110432_raw.fits	29098	2007/06/12	2	1.5	-53.8	100
i61gm304r_07163112321_raw.fits	29099	2007/06/12	2	1.5	-54.0	100
iu013a04r_07180145102_raw.fits	31970	2007/06/29	2	1.5	-78.3	3000
iu013a07r_07180154511_raw.fits	31972	2007/06/29	2	1.5	-78.3	3000
iu013a0ar_07180164207_raw.fits	31974	2007/06/29	2	1.5	-78.1	3000
iu011a07r_07179124042_raw.fits	31919	2007/06/28	2	1.5	-81.6	3000
iu011304r_07181003602_raw.fits	32018	2007/06/29	2	1.0	-78.1	3000
iu011307r_07181013011_raw.fits	32020	2007/06/29	2	1.0	-78.5	3000
iu01130ar_07181022707_raw.fits	32022	2007/06/29	2	1.0	-78.1	3000